

Computerized interferometric surface measurements [Invited]

James C. Wyant

College of Optical Sciences, University of Arizona, 1630 E. University Boulevard, Tucson, Arizona 85721, USA (jcwyant@optics.arizona.edu)

Received 24 September 2012; accepted 25 September 2012;
posted 5 October 2012 (Doc. ID 176778); published 21 December 2012

The addition of electronics, computers, and software to interferometry has enabled enormous improvements in optical metrology. This paper discusses four areas in which computerized interferometric measurement improvements have been made in the measurement of surface shape and surface roughness: (a) The use of computer-generated holograms for the testing of aspheric optics, (b) phase-shifting interferometry for getting interferometric data into a computer so the data can be analyzed, (c) computerized interference microscopes, including multiple-wavelength and coherence scanning, for the precision measurement of surface microstructure, and (d) vibration-insensitive dynamic interferometers for enabling precise measurements in noncontrolled environments. © 2012 Optical Society of America

OCIS codes: 120.0120, 120.3180, 120.3940, 120.5050, 120.6650, 120.6660.

1. Introduction

Computers have changed, and for the most part improved, almost everything we do, and this is especially true in metrology. For example, improved computers, electronics, and software have helped make possible enormous advances in the measurement of surface shape and surface roughness. These measurement enhancements have made possible improvements in the fabrication of precision optics, hard disk drives, machine tools, and semiconductors, to name just a few areas in which improved metrology has been responsible for both improved manufacturing quality and the ability to make components or systems that previously could not be made. This paper reviews some of the computerized optical measurements areas the author has been involved with that have led to improvements in the manufacturing of components or systems. For some of the items discussed, at the time the original work was performed, the measurement techniques were not very useful because the enabling technology, such as plotters,

computers, detector arrays, and computing power, needed to make useful and accurate measurements were not available, but the concepts were sound. When the supporting technology became available, however, the measurement techniques became useful and valuable.

The discussion is divided into four sections for which the improved measurement technique has made a significant improvement in either the fabrication of optics or the manufacturing of other items important in our daily lives: (a) use of computer-generated holograms (CGHs) for the testing of complex aspheric optics; (b) phase-shifting interferometry (PSI) for getting interferometric data into the computer so the data can be analyzed to determine what is wrong with the component or system being measured, how to improve or fix the component or system, and how well the component or system will work if it is not improved; (c) computerized interference microscopes, including multiple-wavelength and coherence scanning, for the measurement of surface microstructure; and (d) vibration-insensitive dynamic interferometers for enabling high-precision interferometric measurements in manufacturing environments in which high-precision surface

measurements previously could not be made, and for the measurement of the change in surface shape of vibrating surfaces.

2. Computer-Generated Holograms

Optics with aspheric surfaces have become essential in high-performance optical systems because they can give improved performance with fewer optical components than if only optics having spherical surfaces are used. Fewer optical components mean reduced weight and generally reduced cost. To produce high-quality aspheric surfaces, the surface shape must be measured, and a CGH is excellent for producing a reference wavefront for measuring the shape of the aspheric surface [1–8]. The CGH can be thought of as a binary representation of the interferogram, or hologram, that would be recorded if we were to interfere the aspheric wavefront coming from a perfect aspheric surface with a reference beam. The procedure for making the CGH is to first ray trace the interferometer to determine the position of the fringes in this theoretical interferogram (hologram). A plotter, such as a laser beam recorder or an e-beam recorder, is then used to draw lines along the calculated fringe positions. Figure 1 shows a simple CGH. Generally, the CGH would be more complicated, but a more complicated one would be too hard to see in the publication.

Figure 2 shows a typical laser-based Fizeau interferometer with a CGH added to test an aspheric surface [4]. A spherical beam illuminates the CGH and several beams are produced: one is an aspheric wavefront that has the property that upon reaching the aspheric mirror under test, it will match the shape of the aspheric surface if the surface is perfect. The beam is reflected back to the CGH and again several beams are produced, of which one is a spherical wave (if the aspheric surface is perfect) that interferes with the spherical wave reflected off of the

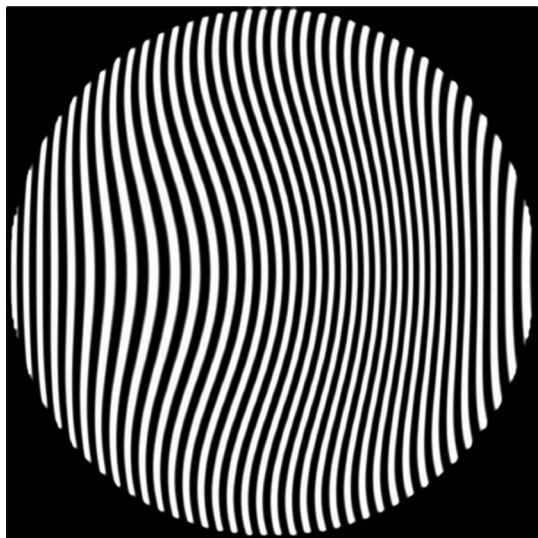


Fig. 1. Typical CGH.

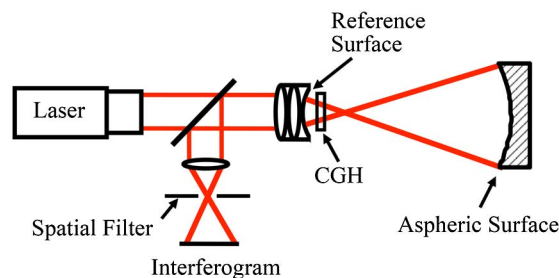


Fig. 2. (Color online) Laser-based Fizeau interferometer with CGH for testing an aspheric surface.

reference surface. The resulting fringes give the error in the aspheric surface being tested.

The largest potential source of error in the CGH test is the wavefront error resulting from the lines (fringes) making up the CGH being in the wrong location [2–4,9–18]. This error is given by the following:

$$\Delta W(x,y) = \lambda \frac{\varepsilon(x,y)}{S(x,y)},$$

where $\varepsilon(x,y)$ is the fringe position error in the direction perpendicular to the fringes, $S(x,y)$ is the localized fringe error, and λ is the wavelength [4]. As an example, let us say the fringe spacing is 20 μm and the fringe position error is 0.1 μm , then a wavefront error of $\lambda/200$ is produced. In the early days of CGH work, wavefront errors produced by plotters were a serious problem and limited the usefulness of CGHs, and many of the early CGH papers measured the quality of plotters and correcting for plotter errors [13]. Now with modern electron-beam or laser plotters, the plotter error is no longer significant. A conservative spec for electron-beam recorders that have been developed by the electronic industry to make electronic chips, but that also can be used to make CGHs, is a positional accuracy of 50 nm over a maximum dimension of 150 mm \times 150 mm for 3 \times 3 million distortion-free resolution points, compared with 1000 \times 1000 for the paper plotters that were used to make the early CGHs [4,13]. Thus, laser recorders and e-beam recorders have the resolution and accuracy required to make high-quality CGHs for testing most state-of-the-art aspheric elements. If the aspheric wavefront being tested is still too complicated for the reference surface to be produced by a CGH by itself, then additional lenses or mirrors can be used with the CGH to produce the required aspheric wavefront for the test [18].

Errors also can result from the hologram being in the wrong location. Lateral misalignment gives errors proportional to the slope of the wavefront [4]. Errors resulting from longitudinal misalignment are less sensitive if the hologram is placed in collimated light, although generally this is not necessary. Generally alignment marks, crosshairs, are placed on the CGH to aid in the alignment. Another good feature of a CGH test is that additional holographic

structures can be placed on the CGH to produce alignment spots for the optical setup. Now that high-quality plotters are available, CGHs are widely used in the testing of aspheric optics.

Using CGHs to test aspheric optics is extremely useful because of the wide variation of aspherics that can be tested. Once you have the software for producing a CGH and access to an electron-beam recorder, it is easy to make a new hologram to test a different aspheric surface. As mentioned, crosshairs can be put on the CGH to aid in the alignment of the CGH and additional holograms can be placed on the CGH to aid in the alignment of the optics. It is impossible to overemphasize the benefit of being able to add additional holograms to the CGH to aid in the alignment of both the CGH and the entire optical test setup. CGH interferometers work well with the phase-shifting techniques described in Section 3.

When the original work describing the use of CGHs for testing aspheric surfaces was performed, the plotters used to make the CGHs were not of sufficient quality to make CGHs to test anything but the simplest aspheres, and the CGH research was useful only to produce papers and talks. Now that high-quality electron-beam recorders are available, CGHs are truly useful for testing state-of-the-art aspheric surfaces, and they are used daily in the manufacturing of sophisticated state-of-the-art optical systems.

3. Phase-Shifting Interferometry

Most optical-testing interferometers now use phase-shifting techniques because phase shifting is a highly accurate rapid way of getting the interferogram information into a computer and the inherent noise in the data-taking process is so low that in a good environment angstrom or subangstrom surface height measurements can be performed. Although the earliest reference to PSI is believed to be 1966 [19], the development and demonstration of PSI began in the 1970s [20–23]. In PSI, the phase difference between the interfering beams is either changed in discrete steps (sometimes called phase-stepping interferometry) or it is changed at a constant rate as the detector is read out [23]. It can be shown that by making three or more measurements of the irradiance of the interference pattern as the phase difference is varied, it is possible to accurately determine the phase difference between the two interfering beams. The most commonly used phase shift between consecutive frames of data is 90 deg because it simplifies the calculations. Generally, more than three phase shifts are used to reduce the requirement for the phase shift being exactly 90 deg [24].

The irradiance of the interference pattern can be written as follows:

$$I(x, y) = I_{dc} + I_{ac} \cos[\phi(x, y) + \alpha(t)],$$

where $\phi(x, y)$ is the phase being measured and $\alpha(t)$ is the phase shift. If four frames of data are taken as the phase changes by 90 deg between readouts,

the irradiance for the four measurements and the measured phase, $\phi(x, y)$, are given by the following:

$$I_1(x, y) = I_{dc} + I_{ac} \cos[\phi(x, y)] \quad \text{if } \phi(t) = 0$$

$$I_2(x, y) = I_{dc} - I_{ac} \sin[\phi(x, y)] \quad \text{if } \phi(t) = \frac{\pi}{2}$$

$$I_3(x, y) = I_{dc} - I_{ac} \cos[\phi(x, y)] \quad \text{if } \phi(t) = \pi$$

$$I_4(x, y) = I_{dc} + I_{ac} \sin[\phi(x, y)] \quad \text{if } \phi(t) = \frac{3\pi}{2}$$

$$\tan[\phi(x, y)] = \frac{I_4(x, y) - I_2(x, y)}{I_1(x, y) - I_3(x, y)}.$$

Although this is a simple equation, it is powerful and an excellent way of getting interferogram data into a computer. As a result of the subtraction and division and performing the calculation at each detector point, the effects of fixed pattern noise and gain variations across the detector are canceled out, as long as the effects are not so large that the dynamic range of the detector becomes too small to be of use.

Once the phase is determined across the interference field, the corresponding height distribution, $h(x, y)$, on the test surface can be determined, as follows:

$$h(x, y) = \frac{\lambda}{4\pi} \phi(x, y),$$

where we have assumed the surface is being measured at normal incidence. Almost all interferometers used to measure surface height variations use phase-shifting techniques.

When the original ideas for PSI were developed, PSI was not practical. Solid-state detector arrays were not yet available; computers were large, expensive, and not as powerful as you would want; and the required electronics were massive. In the late 1960s and early 1970s, building a phase-shifting interferometer was so expensive that classified government projects were some of the only sources of funding available for making active or adaptive optics for satellite reconnaissance systems for which cost was not too important. One of the first systems built had racks of electronics and only 21 discrete detectors, whereas presently PSI systems using inexpensive personal computers and 4 million pixel detector arrays are common. In spite of how complicated and crude the first phase-shifting interferometers were, it was possible to demonstrate the adaptive optics correction of atmospheric turbulence [25]. Fortunately, or unfortunately, this early system worked so well that as soon as it was shown that it worked, the U.S. government classified the work for many years.

4. Computerized Interference Microscopes

In the 1980s, solid-state detector arrays and personal computers became available so it made sense to make commercial phase-shifting interferometers, including phase-shifting interference microscopes for the measurement of surface microstructure. This section describes a computerized interferometric microscope system for the measurement of surface microstructure for which a repeatability of the surface height measurements of less than 0.1 nm can be obtained for smooth surfaces, and by using multiple-wavelength and coherence-scanning techniques, surfaces with height variations larger than hundreds of micrometers can be measured to within an accuracy of a few nanometers.

Figure 3 shows a simplified schematic of the instrument [26–28]. The configuration shown in the figure utilizes a two-beam Mirau interferometer at the microscope objective. In the figure, a tungsten halogen lamp is used as the light source, although LEDs are currently more common. In the phase-shifting mode of operation, a spectral filter of 40 nm bandwidth centered at 650 nm is used to increase the coherence length. For the vertical-scanning mode of operation described in this section, the spectral filter is not used. Light reflected from the test surface interferes with light reflected from the reference. The resulting interference pattern is imaged onto the CCD array. The output of the CCD is digitized and read by the computer. The Mirau interferometer is mounted on either a piezoelectric transducer or a motorized stage so that it can be moved vertically. During this movement, the distance from the lens to the reference surface remains fixed. Thus, a phase shift is introduced into one arm of the interferometer. By introducing a phase shift into only one arm while recording the interference pattern that is produced, it is possible to perform either the phase-shifting technique previously described or the vertical-scanning coherence sensing technique described next.

In the phase-shifting mode of operation, the phase is obtained by calculating the arc tangent that gives the phase modulo 2π , and hence discontinuities may be present in the calculated phase. These 2π discontinuities can be removed as long as the slopes on the

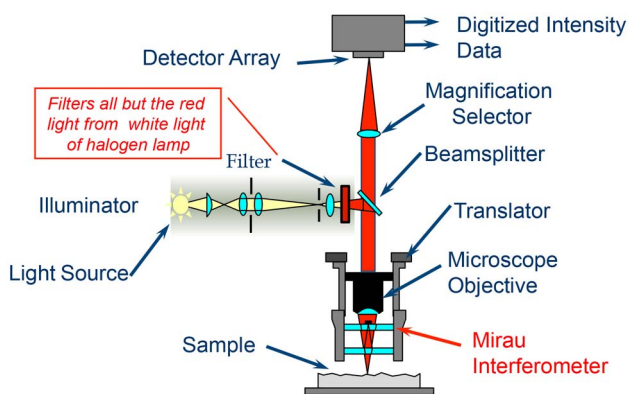


Fig. 3. (Color online) Computerized interference microscope.

sample being measured are limited so that the actual phase difference between adjacent pixels is less than π (surface height must change by less than a quarter-wavelength). The dynamic range can be increased by performing the measurement at two or more wavelengths [29–31].

In two-wavelength interferometry, phase measurements are performed at two different wavelengths, and the two-phase measurements are subtracted. Assuming no chromatic aberration is present, the result is equivalent to performing a single wavelength at a longer equivalent wavelength given by the product of the two wavelengths divided by the difference. This can be seen as follows:

$$\begin{aligned} \text{phase}_{\lambda_2} - \text{phase}_{\lambda_1} &= 2\pi \left(\frac{1}{\lambda_2} - \frac{1}{\lambda_1} \right) \text{OPD} \\ &= \frac{2\pi}{\lambda_{\text{eq}}} \text{OPD}, \quad \text{where} \\ \lambda_{\text{eq}} &= \frac{\lambda_2 \lambda_1}{\text{Abs}[\lambda_2 - \lambda_1]}. \end{aligned}$$

The maximum surface slope that can be measured is still a quarter-wavelength between adjacent detector points, but now it is a quarter of the equivalent wavelength, not a quarter of the individual shorter wavelengths. Thus, the dynamic range of the measurement is increased by the ratio of the equivalent wavelength to the individual single wavelength. Unfortunately, the noise is increased by the same ratio. It is easy to get around this increased noise when steps are being measured. The single-wavelength measurements are correct, except the step heights are off by an integer number of half-wavelengths. The errors in the step heights can be corrected by comparing the heights measured using the equivalent wavelength with the heights measured using the single wavelength, and then by adding or subtracting an integer number of half-wavelengths to the heights measured using the single wavelength, so that the difference between the single wavelengths and the equivalent wavelength is less than a quarter-wave. In this way, it is possible to obtain the dynamic range of the equivalent wavelength and the accuracy of the single-wavelength measurement.

Often, a better way to increase the dynamic range of an interference microscope is to use coherence scanning [32–34]. In the coherence-scanning mode of operation, an unfiltered white light source is used. Because of the large spectral bandwidth of the source, the coherence length of the source is short, and good contrast fringes will be obtained only when the two paths of the interferometer are closely matched in length. Thus, if in the interference microscope the path length of the sample arm of the interferometer is varied, the height variations across the sample can be determined by looking at the scan position for each sample point for which the fringe contrast is a maximum. In this measurement, there are no height ambiguities, and because in a properly

adjusted interferometer the sample is in focus when the maximum fringe contrast is obtained, there are no focus errors in the measurement of surface microstructure. In the vertical-scanning mode, nearly any type of surface can be measured as long as the reflected light gets back through the microscope objective. Although almost any surface can be measured, however, there may be errors in the measurement and care is required. For example, if a very rough surface is measured, there may be multiple reflections of the light in the surface structure, resulting in errors in the surface measurement [35,36]. In spite of this potential problem, the coherence-scanning interference microscope is widely used in a wide variety of industries, including magnetic data storage, semiconductor, machine tool, biomedical, and so on.

The ideas of coherence scanning go back to the days of Michelson, but it was not until the 1990s that the required detectors and computers were available to make a practical commercial system [34]. The early commercial systems used digital signal processors (DSPs) to perform the required calculations to simultaneously determine the coherence calculations at all detector points. Personal computers later became powerful enough to do the calculations without DSPs, and since then, as computers became faster and faster, it became easier to do the calculations at a million or more data points at vertical scan speeds of greater than 25 $\mu\text{m/s}$.

5. Vibration-Insensitive Dynamic Interferometers

PSI is extremely useful for the testing of optics, but in many situations, especially for the testing of large telescope optics, or in manufacturing environments, the environment limits the measurement accuracy and sometimes the environment is sufficiently bad that the measurement cannot be performed. This section describes a technique for reducing effects of vibration by using dynamic (single-shot) interferometry techniques. The single-shot interferometer described is insensitive to vibration, and many measurements can be averaged to reduce the effects of air turbulence and enable the precision measurement of large optical components. Also, if surface shape is changing with time, the changes in surface shape can be measured and movies can be made showing how the surface shape changes as a function of time.

As stated, in conventional temporal PSI three or more interferograms are obtained for which the phase difference between the two interfering beams changes by 90 deg between consecutive interferograms. The major effect of vibration in temporal PSI is that the vibration results in incorrect phase changes between consecutive interferograms. Vibration effects can be reduced if all of the phase-shifted frames are taken simultaneously, and fortunately, there are several ways to obtain all of the phase-shifted frames simultaneously [37–45]. A phase-shifting technique that works well with multiple wavelengths, or even white light, involves the use of a quarter-wave plate (QWP) followed by linear

polarizers at different angles. For this technique, the phase shift between the two interfering beams is nearly independent of wavelength. The QWP is oriented to convert one of the two interfering beams into left-handed circular polarization and the other interfering beam into right-handed circular polarization. If these circularly polarized beams are transmitted through a linear polarizer, a phase shift is shown between the two interfering beams proportional to twice the rotation angle of the polarizer results [46]. See Fig. 4(a).

Thus, if a phase mask is made of an array of four linear wire-grid polarizer elements having their transmission axes at 0, 45, 90, and 135 deg as shown in Fig. 4(b), where a polarizer element is placed over each detector element, the mask will produce an array of four 0, $\pi/2$, π , and $3\pi/2$ deg phase-shifted interferograms. The size of the polarizer elements must be equal to the size of the pixels making up the detector array. Figure 4(c) shows a scanning electron microscope (SEM) photo of the patterned polarizers. The following subsection shows how this polarizer array can be used with both Twyman–Green and

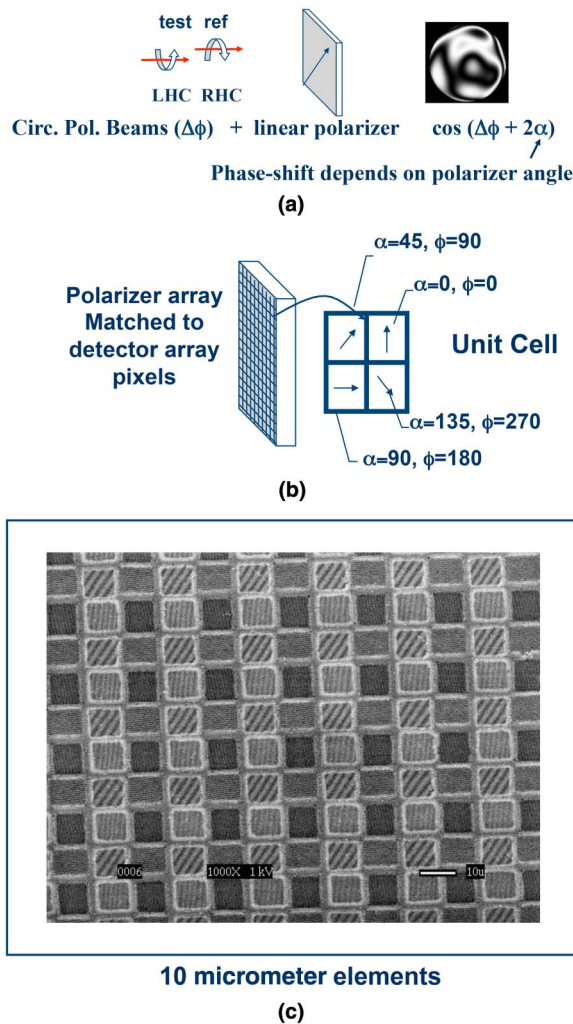


Fig. 4. (Color online) (a) Use polarizer as phase shifter. (b) Array of oriented micropolarizers. (c) SEM of patterned polarizers.

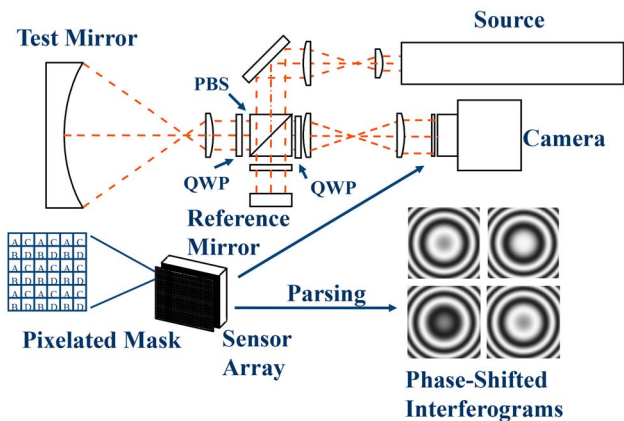


Fig. 5. (Color online) Twyman-Green interferometer with pixelated polarizer array phase shifting.

Fizeau interferometers. This spatial phase-shifting technique does slightly reduce the spatial resolution of the interferometer, but the effect on the spatial transfer function is small [47]. Although it has been known for a long time that rotating a polarizer in a circularly polarized beam changes the phase of the beam, it is only within the past few years that it has been possible to produce the required wire-grid polarizer array to work in the visible spectrum.

A. Simultaneous (Single-Shot) Twyman-Green interferometer

It is fairly easy to make a Twyman-Green interferometer using the micropolarizer phase-shifting

array, and one possible arrangement is shown in Fig. 5. The essential characteristics of the two-beam interferometer are that the test and reference beams have orthogonal polarization and the size of the micropolarizer array matches the CCD array. In Fig. 5, the polarization beam splitter (PBS) sends one state of polarization to the reference arm and the orthogonal state to the test arm. A QWP is placed in each arm, and after the light passes through each QWP twice, the direction of polarization is rotated 90 deg and the beam that was reflected by the PBS on the first pass will be transmitted on the second pass, and the beam that was transmitted on the first pass will be reflected on the second pass. The QWP placed in the output beam converts the orthogonally polarized test and reference beams into left-handed and right-handed circularly polarized beams.

Using this interferometer, it is possible to have the optics under test and the interferometer on different tables without any vibration isolation. By averaging several frames of data, the effects of air turbulence can be minimized. If a surface is vibrating, it is possible to determine precisely how the surface is vibrating. Movies can be made showing how the shape of the vibrating surface is changing in time. Figure 6 shows an array of surface measurements made of a disk vibrating at a frequency of 408 Hz.

B. Single-Shot Laser-Based Fizeau Interferometer

A single-shot laser-based Fizeau interferometer is more difficult to construct than a Twyman-Green

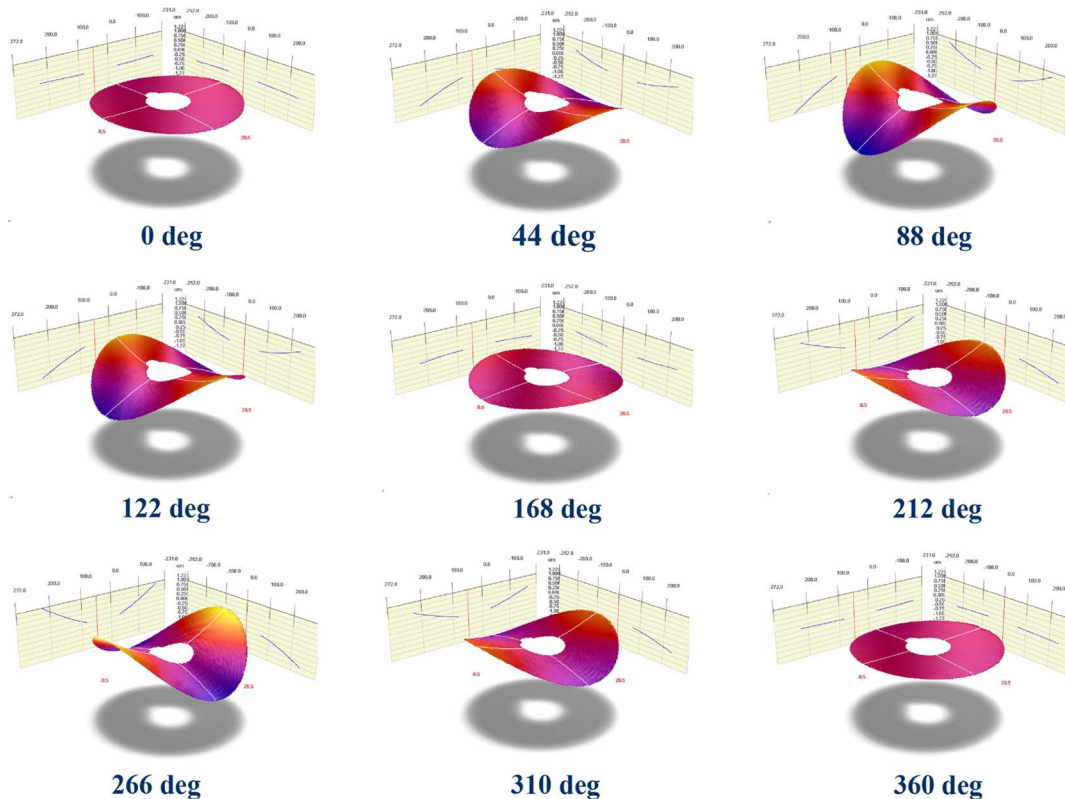


Fig. 6. (Color online) Surface vibrating at frequency of 408 Hz.

interferometer because the Fizeau interferometer is more common path, and it is hard to obtain a reference and test beam having orthogonal polarization. In principle, a QWP can be placed between the test and reference surfaces to rotate the direction of polarization of the test beam by 90 deg, but in practice this does not work well, especially for testing spherical optics. Techniques for which the reference and test beams are tilted with respect to each other have been described [48]. Using tilted beams in any interferometer introduces aberrations, however, because the beams are going through the interferometer elements off-axis. Thus, the biggest advantage of using a Fizeau interferometer is lost—namely, that in a Fizeau interferometer, both test and reference beams transverse the same paths in the interferometer so that errors in the interferometer optics are common to both the test and reference beams, and cancel out. A better approach is the on-axis approach shown in Fig. 7 [49]. This approach also has the great capability that a short-coherence light source can be used, and fewer interference fringes will result from the interference of undesired reflected beams. Thus, a large source of error, the spurious interference fringes often present in interferometers using long-coherence light sources, are eliminated.

In the interferometer shown in Fig. 7, a short-coherence light source is used. The source beam consists of two-path-delayed orthogonally polarized beams. The path difference between the two beams is set equal to the path difference in the Fizeau cavity. The desired interference results from the long-path source beam reflected off the reference surface and the short-path light source beam reflected off the test surface. All beams are on-axis so off-axis aberrations are not a problem. Because both source beams are reflected off both test and reference surfaces and only the two-path-length matched beams give interference, the fringe contrast is reduced, but it is still more than adequate. Because a short-coherence light source is used, spurious fringes are greatly reduced. One source that works well is a modulated diode with coherence length of approximately 300 μm .

This interferometer shown in Fig. 7 can be used for testing windows having nearly parallel surfaces. If a long-coherence source is used, spurious fringes are

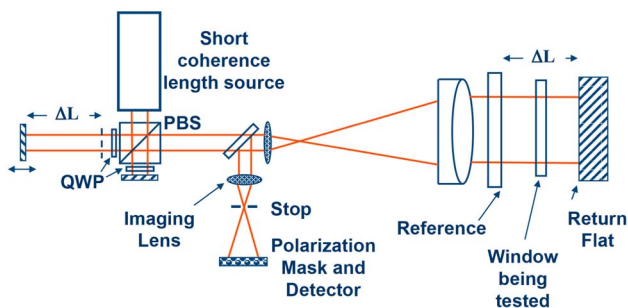


Fig. 7. (Color online) Testing glass sample in transmission or testing each surface in reflection.

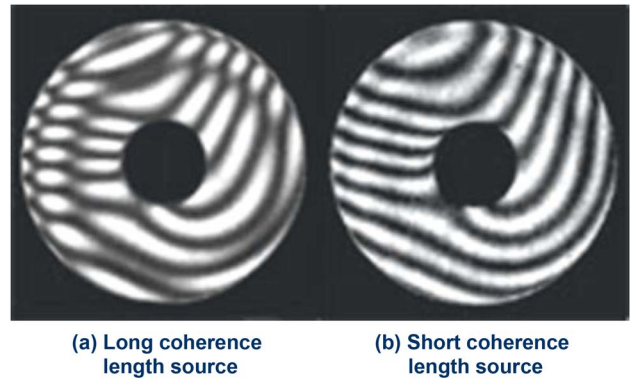


Fig. 8. (Color online) Interference fringes obtain testing a thin glass plate.

obtained as shown in Fig. 8(a); however, with the short-coherence source, interferometer spurious fringes are eliminated, as shown in Fig. 8(b), and by selecting the proper ΔL in the source, it is possible to look at the fringes for reflection off the first surface or the second surface.

A single-shot dynamic interferometer can go a long way toward reducing the effects of what is often a large source of error in PSI, namely, vibration. Averaging many frames of data obtained using a single-shot dynamic interferometer can reduce errors resulting from air turbulence. Averaging data frames in the presence of vibration will average out the double-frequency errors common in PSI [24], and generally more accurate results can be obtained in the presence of vibration than normally can be obtained using conventional temporal PSI in the absence of vibration. Also, it is possible to measure a vibrating surface to determine precisely how the surface is vibrating, and movies can be made showing how the vibrating surface shape changes. Once a person works with a simultaneous dynamic phase-shifting interferometer, it is hard to go back to working with a temporal phase-shifting interferometer.

6. Conclusion

This paper gives four examples of instances in which the addition of electronics, computers, and software to well-known interferometry techniques has provided enormous improvements in optical metrology. When the initial work was performed for most of the examples, the techniques were not particularly useful because the necessary enabling technology was not yet available. The concepts were sound, however, and when the supporting technology became available, the measurement techniques became useful and valuable. This is true in all areas of research, and just because a particular concept is not currently useful, it does not mean that it will never be useful.

References

1. H. D. Polster, J. Pastor, R. M. Scott, R. Crane, P. H. Langenbeck, R. Pilston, and G. Steinberg, "New developments in interferometry," *Appl. Opt.* **8**, 521–556 (1969).
2. J. C. Wyant and A. J. MacGovern, "Computer generated holograms for testing aspheric optical elements," *Applications*

de L'Holographie, Laboratoire de Physique Generale et Optique (Universite de Besancon, 1970), pp. 13–18.

3. A. J. MacGovern and J. C. Wyant, "Computer generated holograms for testing optical elements," *Appl. Opt.* **10**, 619–624 (1971).
4. J. C. Wyant and V. P. Bennett, "Using computer generated holograms to test aspheric wavefronts," *Appl. Opt.* **11**, 2833–2839 (1972).
5. D. Malacara, K. Creath, J. Schmit, and J. C. Wyant, "Testing of aspheric wavefronts and surfaces," in *Optical Shop Testing*, D. Malacara, ed. (Wiley, 2007), pp. 477–488.
6. B. Dorband and H. J. Tiziani, "Testing aspheric surfaces with computer generated holograms: analysis of adjustment and shape errors," *Appl. Opt.* **24**, 2604–2611 (1985).
7. J. Schwider, "Interferometric tests for aspherics," in *Fabrication and Testing of Aspheres*, M. Taylor, M. Piscotty, and A. Lindquist, eds., Vol. **24** of OSA Trends in Optics and Photonics (Optical Society of America, 1999), paper T3.
8. C. Pruss, S. Reichelt, H. J. Tiziani, and W. Olsen, "Computer-generated holograms in interferometric testing," *Opt. Eng.* **43**, 2534–2540 (2004).
9. P. Zhou and J. H. Burge, "Fabrication error analysis and experimental demonstration for computer-generated holograms," *Appl. Opt.* **46**, 657–663 (2007).
10. A. F. Fercher, "Computer-generated holograms for testing optical elements: error analysis and error compensation," *Opt. Acta* **23**, 347–365 (1976).
11. A. Ono and J. C. Wyant, "Plotting errors measurement of CGH using an improved interferometric method," *Appl. Opt.* **23**, 3905–3910 (1984).
12. A. Ono and J. C. Wyant, "Aspherical mirror testing using a CGH with small errors," *Appl. Opt.* **24**, 560–563 (1985).
13. J. C. Wyant, P. K. O'Neill, and A. J. MacGovern, "Interferometric method of measuring plotter distortion," *Appl. Opt.* **13**, 1549–1551 (1974).
14. M. Beyerlein, N. Lindlein, and J. Schwider, "Dual-wave-front computer-generated holograms for quasi-absolute testing of aspherics," *Appl. Opt.* **41**, 2440–2447 (2002).
15. S. Reichelt, C. Pruss, and H. J. Tiziani, "Absolute interferometric test of aspheres by use of twin computer-generated holograms," *Appl. Opt.* **42**, 4468–4479 (2003).
16. S. M. Arnold and R. Kestner, "Verification and certification of CGH aspheric nulls," *Proc. SPIE* **2536**, 117–126 (1995).
17. Y.-C. Chang and J. H. Burge, "Error analysis for CGH optical testing," *Proc. SPIE* **3782**, 358–366 (1999).
18. J. C. Wyant and P. K. O'Neill, "Computer generated hologram: null lens test of aspheric wavefronts," *Appl. Opt.* **13**, 2762–2765 (1974).
19. P. Carré, "Installation et utilisation du comparateur photo-electrique et Interferentiel du Bureau International de Poids et Mesures," *Metrologia* **2**, 13–23 (1966).
20. R. Crane, "Interference phase measurement," *Appl. Opt.* **8**, 538–542 (1969).
21. J. C. Wyant, "Double frequency grating lateral shear interferometer," *Appl. Opt.* **12**, 2057–2060 (1973).
22. J. H. Bruning, D. R. Herriott, J. E. Gallagher, D. P. Rosenfeld, A. D. White, and D. J. Brangaccio, "Digital wavefront measuring interferometer for testing optical surfaces and lenses," *Appl. Opt.* **13**, 2693–2703 (1974).
23. J. C. Wyant, "Use of an ac heterodyne lateral shear interferometer with real-time wavefront correction systems," *Appl. Opt.* **14**, 2622–2626 (1975).
24. J. Schwider, R. Burow, K.-E. Elssner, J. Grzanna, R. Spolaczyk, and K. Merkel, "Digital wave-front measuring interferometry: some systematic error sources," *Appl. Opt.* **22**, 3421–3432 (1983).
25. J. W. Hardy, J. Feinleib, and J. C. Wyant, "Real time phase correction of optical imaging systems," presented at OSA Topical Meeting on Optical Propagation through Turbulence, Boulder, Colorado, 9–11 July 1974.
26. B. Bhushan, J. C. Wyant, and C. L. Koliopoulos, "Measurement of surface topography of magnetic tapes by Mirau interferometry," *Appl. Opt.* **24**, 1489–1497 (1985).
27. J. C. Wyant, "Optical profilers for surface roughness," *Proc. SPIE* **525**, 174–180 (1985).
28. J. C. Wyant and K. Creath, "Advances in interferometric optical profiling," *Int. J. Mach. Tools Manufact.* **32**, 5–10 (1992).
29. J. C. Wyant and K. Creath, "Two-wavelength phase-shifting interferometer and method," U.S. patent 4,832,489 (23 May 1989).
30. Y.-Y. Cheng and J. C. Wyant, "Two-wavelength phase shifting interferometry," *Appl. Opt.* **23**, 4539–4543 (1984).
31. Y.-Y. Cheng and J. C. Wyant, "Multiple-wavelength phase-shifting interferometry," *Appl. Opt.* **24**, 804–807 (1985).
32. M. Davidson, K. Kaufman, I. Mazor, and F. Cohen, "An application of interference microscopy to integrated circuit inspection and metrology," *Proc. SPIE* **775**, 233–247 (1987).
33. T. Dresel, G. Hausler, and H. Venzke, "Three-dimensional sensing of rough surfaces by coherence radar," *Appl. Opt.* **31**, 919–925 (1992).
34. P. J. Caber, "An interferometric profiler for rough surfaces," *Appl. Opt.* **32**, 3438–3441 (1993).
35. F. Gao, R. K. Leach, J. Petzing, and J. M. Coupland, "Surface measurement errors using commercial scanning white light interferometers," *Meas. Sci. Technol.* **19**, 015303 (2008).
36. R. K. Leach, C. L. Giusca, and J. M. Coupland, "Advances in calibration methods for micro- and nanoscale surfaces," *Proc. SPIE* **8430**, 84300H (2012).
37. M. Takeda, H. Ina, and S. Kabayashi, "Fourier-transform method of fringe-pattern analysis for computer-based topography and interferometry," *J. Opt. Soc. Am.* **72**, 156–160 (1982).
38. K. H. Womack, "Interferometric phase measurement using spatial synchronous detection," *Proc. SPIE* **429**, 8–15 (1983).
39. O. Y. Kwon, "Multichannel phase shifted interferometer," *Opt. Lett.* **9**, 59–61 (1984).
40. C. L. Koliopoulos, "Simultaneous phase-shift interferometer," *Proc. SPIE* **1531**, 119–128 (1991).
41. M. Takeda, Q. Gu, M. Kinoshita, H. Takai, and Y. Takahashi, "Frequency-multiplex Fourier-transform profilometry: a single shot three-dimensional shape measurement of objects with large height discontinuities and/or surface isolations," *Appl. Opt.* **36**, 5347–5354 (1997).
42. J. Millerd, N. Brock, J. Hayes, M. North-Morris, M. Novak, and J. C. Wyant, "Pixelated phase-mask dynamic interferometer," *Proc. SPIE* **5531**, 304–314 (2004).
43. J. E. Millerd, N. J. Brock, J. B. Hayes, and J. C. Wyant, "Instantaneous phase-shift, point-diffraction interferometer," *Proc. SPIE* **5531**, 264–272 (2004).
44. M. Novak, J. Millerd, N. Brock, M. North-Morris, J. Hayes, and J. C. Wyant, "Analysis of a micropolarizer array-based simultaneous phase-shifting interferometer," *Appl. Opt.* **44**, 6861–6868 (2005).
45. N. Brock, J. Hayes, B. Kimbrough, J. Millerd, M. North-Morris, M. Novak, and J. C. Wyant, "Dynamic interferometry," *Proc. SPIE* **5875**, 58750F (2005).
46. S. Suja Helen, M. P. Kothiyal, and R. S. Sirohi, "Achromatic phase-shifting by a rotating polarizer," *Opt. Commun.* **154**, 249–254 (1998).
47. B. Kimbrough and J. Millerd, "The spatial frequency response and resolution limitations of pixelated mask spatial carrier based phase shifting interferometry," *Proc. SPIE* **7790**, 77900K (2010).
48. D. M. Sykora and P. de Groot, "Instantaneous measurement Fizeau interferometer with high spatial resolution," *Proc. SPIE* **8126**, 812610 (2011).
49. B. Kimbrough, J. Millerd, J. Wyant, and J. Hayes, "Low coherence vibration insensitive Fizeau interferometer," *Proc. SPIE* **6292**, 62920F (2006).